Improving Grasping Performance of Underactuated Two Finger Robotic Hands Using Variable Stiffness

Dylan Denizon, Sedat Dogru, Lino Marques, *Member, IEEE*
Institute of Systems and Robotics
Department of Electrical and Computer Engineering
University of Coimbra
3030-290 Coimbra, Portugal
Email: {dylan.denizon, sedat, lino}@isr.uc.pt

***Abstract*—In this work, we aim to improve the performance of an underactuated anthropomorphic tendon driven robotic gripper with two fingers by allowing the stiffness of the finger joints to change as a function of the object shape. An optimization problem requiring that the gripper apply a constant total contact force with a minimum actuation force was formulated using a Genetic Algorithm (GA) approach in order to obtain a set of designs with geometrical parameters such as position and size of various elements of the fingers as well as stiffness of the joints. The optimization process was also repeated for the fixed stiffness case to compare the two approaches, demonstrating that the addition of variable stiffness allowed to achieve the same grasp with less actuation force.**

***Index Terms*—Underactuated gripper, Variable stiffness, Optimization, Genetic Algorithm**

I. Introduction

Robotic grippers have revolutionized various industries by allowing robots to grasp, hold, and manipulate objects with different shapes, sizes, and materials [1], [2]. To be able to grasp this wide range of objects, different types of grippers have been designed over time, varying actuation methods (vacuum, tendon-based, adaptive), the configuration and number of fingers, and stiffness [3]. Tendon driven grippers are often preferred due to their intrinsic anthropomorphic characteristics and improved weight to size ratio. However, with increasing number of tendons, controlling such grippers becomes more difficult and more complex [4]. In order to solve this problem, underactuated robotic grippers were proposed [5]. These grippers can achieve the same movements with fewer tendons, in some configurations.

Designing underactuated robotic grippers requires taking into account the grasp type and the object shape, and proper modeling and optimization of certain system parameters. These can be achieved using various optimization approaches such as Genetic Algorithms (GA) or Reinforcement Learning (RL) [6], [7]. Zhang et al. [8] have developed a RL based computational framework that changes the number of fingers, the number of links, and the position of the fingers. Treratanakulwong et al. [9] reduced the friction loss over tendon path by routing it through 3D pulleys, while Boisclair et al. [10] reduced the contact losses between the phalanges by introducing rolling contact joints instead of the traditional revolute joints. Yoon et al. [11] proposed a design controlled by two tendons where the finger can elongate to increase the task space.

Underactuated grippers allow achieving different grasps, such as pinching and enveloping, using the same gripper design. Hussain et al. [12] demonstrated that by setting specific stiffness values on the joints, pre-formed shapes could be achieved with the fingers using a single tendon. Yang et al. [13] showed that different grasping configurations could be achieved by optimizing the torsion spring parameters of the joints using a co-optimization approach that takes into account grasping skills and structural parameters. On the other hand, Zhang et al. [14] showed that grasp shape could be modified using two tendons with different winding paths, with the tendons aiming to change the resulting moment of the end knuckle's revolute joint.

Another approach is to allow dynamic changes in the intrinsic parameters of the gripper in order to make it adapt to the object. Mizushima et al. [15] developed a gripper based on jamming transition that allows the gripper to adapt its rubber skin to the shape of the object. Additionally, the grasping posture can be fixed by applying vacuum so that the object can be grasped more firmly and stably. Wang et al. [16] demonstrated that by using a finger structure where the segments could change their own structural stiffness to allow variable bending length in order to conform objects with different sizes, the performance was improved compared with fixed length grippers. On the other hand, different grasping shapes can be achieved by changing the stiffness of the finger joints, as shown by Yang et al. [17].

In order to design a gripper that satisfies multiple requirements, several parameters have to be taken into account at the same time. Ciocarlie et al. [18], aiming to grasp a diverse set of objects, proposed a design that optimizes the length of the links, the entry and exit points of the tendons through the phalanges, and the stiffness and radius of the joints, using a data-driven approach. Dong et al. [19] optimized the geometric

This work is financially supported by national funds through the FCT/MCTES (PIDDAC), under the project PTDC/CTA-AMB/3489/2021 "RECY-SMARTE - Sustainable approaches for recycling discarded mobile phones", and by AM2R project "Mobilizing Agenda for business innovation in the Two Wheels sector" funded by PRR - Recovery and Resilience Plan and by the Next Generation EU Fund, under reference C644866475-00000012 | 7253.

parameters of two fingers, each with three phalanges. The parameters were the phalange lengths and widths, the radii of the joints, the palm width, and the positions of the six pulleys used to modify the tendon route.

Surveying optimization studies on underactuated robotic hand design, we notice two different approaches that are mostly used by the research community. In the first approach, the physical design is analytically described using equations [6], whereas in the second, simulation is used [20]. Our literature survey had revealed that no work had been proposed that use a data-driven approach to optimize the position of the joints relative to the phalanges and the starting angle of the fingers, in addition to other design variables. Hence, we recently studied the optimization of both geometric and mechanical design parameters of an underactuated robotic gripper with two fingers, taking into account these missing variables [21]. In the optimization process, we optimized 21 variables of the chosen design, which are length, width and distances between the successive phalanges; the location, size and stiffness of each joint rotation point; the distance between the joints and tendons; and finally, the starting angle of the fingers. However, in [21] we assumed a fixed stiffness for all objects. In this work, we relax this requirement and propose varying the fitness based on the object that the robotic hand is going to grasp, hence increasing the number of optimization variables to include stiffness for different grasps. Due to the high number of variables in the optimization, we use a GA based approach that optimizes the contact forces using data obtained from grasp simulations.

The rest of the paper is organized as follows. In the next section, we first present the gripper model used in the design optimization, and then present the specifications of the Genetic Algorithm. In section III, we present the experimental results, concluding the paper in section IV.

II. Methods

The goal in this work is to improve the performance of our previous robotic gripper [21] while maintaining the same model. The gripper consisted of two underactuated fingers with anthropomorphic characteristics. It was made of phalanges that were connected by joints and actuated by tendons. In previous work we demonstrated that by optimizing the geometric dimensions and the stiffness of the joints, which stay the same for different grasping strategies, the gripper could perform stable flat pinching and enveloping grasps while maximizing the contact forces.

In order to improve the performance while keeping the same model, the parameters should be allowed to change between the different grasps. Since geometrical changes in real-time would be difficult, the stiffness of the joints remains as the only real-time variable. The stiffness, S, used in the paper is defined by the following equation:

$$S = \frac{\tau}{\theta}, \tag{1}$$

where τ correspond to the torque applied on the joints and θ to the angle of rotation of the joints. Changing the stiffness allows us to change the torque needed to rotate to a specific angle. In real case scenarios, the way stiffness is tuned will depend on the technology used to implement stiffness, with some example technologies being Shape Memory Alloy (SMA) wires, springs, motors, etc.

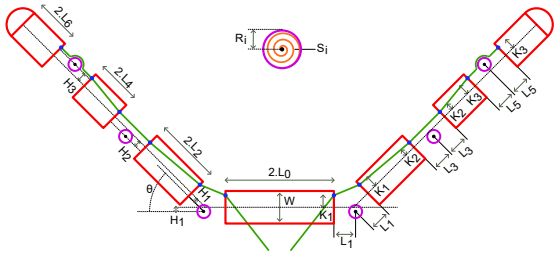

Fig. 1: A schematic of the optimized hand with respective design parameters. The green line represents the tendons and the red boxes represent the phalanges. The magenta circles with the black dots represent the joints.

Below, we present the method used to improve the performance of the gripper by allowing the stiffness of the joints to change between different grasps.

A. Gripper model

Considering our requirement, we maintained our previous geometric model of the gripper as presented in Fig. 1, in which it can be seen that the design has two symmetrical fingers with three phalanges each, driven by tendons. The geometries around each rotational joint are locally symmetric to simplify the model, reducing the number of design parameters to a total of 21, which are described next. The lengths are given by L_i ($i \in \{0, ..., 6\}$) where L_2, L_4 and L_6 denote the half phalange lengths, L_0 denotes the half-length of the palm, and L_1, L_3, L_5 denote the distance between the phalanges and the points of rotation of the joints. R_1, R_2, R_3, H_1, H_2, H_3, S_1, S_2 and S_3 denote the radii, the heights relative to the center of the phalanges, and the stiffnesses of the three joints respectively. θ denotes the starting angle of the first phalange relative to the palm. K_1, K_2 and K_3 denote the distances of the virtual pulleys, which guide the tendons in and out of the phalanges, to the centerline. Finally, W represents the width of the phalanges. The tendon route will always be a straight line between the virtual pulleys (i.e. ends of the phalanges) except when the line passes around the circle of the joints, in which case the tendon will wrap around it. In order to allow changes of the stiffness between grasps, the stiffness variable, S_i, was changed to S_{Ei} for the enveloping grasp and S_{Pi} for the pinching grasp, increasing the number of variables to a total of 24.

Let $\vec{x} = (L_{[0..6]}, R_{[1..3]}, H_{[1..3]}, S_{E[1..3]}, S_{P[1..3]}, K_{[1..3]}, \theta)$ be the variable vector with respect to which the optimization will be done. Let F_s ($s \in \{0, L_1, L_2, L_3\}$) stand for the normal force of the respective surface s. Let $\vec{F} = (F_0, F_{L_1}, F_{L_2}, F_{L_3})$ be the force vector (variable) containing all the contact forces and F_A be the actuation force in both tendons. Let $\sigma(\,.\,)$ denote the standard deviation functions of their arguments. Similarly,

let $\vec{F}(\,.\,)$ be the value of the force vector when grasping its argument. Let L_F be the length of the finger, measured from the tip of the finger to the joint connecting it to the palm. Hence

$$L_F = L_1 + 2L_2 + 2L_3 + 2L_4 + 2L_5 + 2L_6 \tag{2}$$

B. Problem Formulation

Grasping requires the phalanges to apply force on the objects. This force is indirectly applied by pulling the tendons downward. However, the required amount of force depends on the type of object, amount of friction between the surfaces and even the orientation of the hand with respect to gravity.

In order to simplify the force calculation we assumed that the amount of friction between the surfaces is high enough that the object does not slip between the fingers, hence we consider only the normal forces in the model. However, we think that it is important to distribute the force uniformly across the different surfaces of the gripper, and hence we set the goal as to minimize the actuation force, F_A, and the standard deviation of the contact forces, $\sigma(F_0 + F_{L_1} + F_{L_2} + F_{L_3})$, for a constant contact force, $\vec{F}$, (formulated as $||\vec{F}| - F_{\mathrm{C}}| < \varepsilon$ with $F_{\mathrm{C}} = 2\,\mathrm{N}$ in the optimizer) for both grasping strategies. This approach also allows to increase the contact to actuation force ratio, reducing the effort on the motor, eventually providing a more efficient system.

The solution clearly has to obey some sets of constraints. The first set of constraints that is defined for the model concerns the lower and upper limits, ($\vec{x}_L$, $\vec{x}_U$), for the geometric parameters, $\vec{x}$, as shown on Table I, as well as a maximum acceptable length for the fingers ($L_{\text{FINGER MAX}} = 120\,\mathrm{mm}$). The second set of constraints is related to the contact between the test objects and the phalanges. For the enveloping grasp it was desired that at least the last two phalanges and the palm make contact with a minimum force of $F_{\text{MIN CONTACT}} = 0.4\,\mathrm{N}$, and for the pinching grasp, the constraints are the same excluding the palm, which is not required to contact the object.

For optimization, a cylinder with a radius of $4\,\mathrm{cm}$ and a prism with $3\,\mathrm{cm}$ of width and $5\,\mathrm{cm}$ of length were chosen, using the first for the enveloping grasp and the second for the flat pinching grasp. These shapes favor the mentioned grasping, as can be seen from the representation of the contact points between the fingers and objects in Fig. 2. The cylinder is a good approximation to bottles and cups that the gripper would be expected to grasp, and the prism approximates other prismatic objects such as books, boxes, laptops, etc.

The resulting optimization problem for enveloping and flat pinching grasps can be defined as follows:

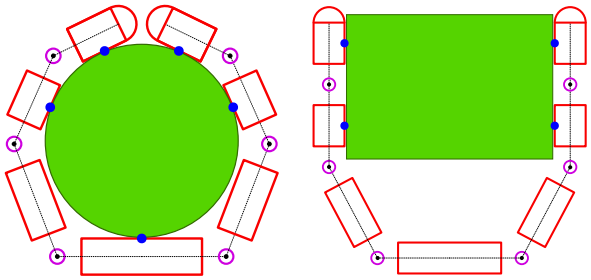

(a) (b)

Fig. 2: A schematic of the hand grasping a circular (a) and a rectangular (b) object. The blue dots represent the contact points, which also correspond to the locations of the force sensors used in the simulation. The tendons are not shown to reduce image clutter.

$$\begin{aligned}
\text{minimize } f_1(\vec{x}) &= F_A(\text{Box})\,, && (3)\\
f_2(\vec{x}) &= F_A(\text{Cylinder})\,, && (4)\\
f_3(\vec{x}) &= \sigma(\vec{F}(\text{Box}))\,, && (5)\\
f_4(\vec{x}) &= \sigma(\vec{F}(\text{Cylinder}))\,, && (6)\\
\text{subject to } L_F &\leq L_{\text{FINGER MAX}}\,, && (7)\\
F_{L_i} &\geq F_{\text{MIN CONTACT}} \;\; i \in \{2,3\}\,, && (8)\\
F_0 &\geq F_{\text{MIN CONTACT}} \text{ for cylinder}\,, && (9)\\
||\vec{F}| - F_{\mathrm{C}}| &\leq \varepsilon\,, && (10)\\
\vec{x}_L \leq \vec{x} &\leq \vec{x}_U\,. && (11)
\end{aligned}$$

Note in the above formulation that the constraint on F_0 is checked only for the cylinder object, i.e. the enveloping grasp. Above it can be seen that the constraints are defined only on the left finger, because the gripper and the objects have symmetric shapes, and hence the forces on the left and the right fingers are expected to be the same. This symmetry assumption allowed to reduce the number of constraints by half, simplifying the optimization algorithm.

C. Solution

The above presented optimization problem requires the optimization of 4 functions with respect to several constraints and the 24 variables, which is difficult to track and perform analytically using for example a gradient descent based approach. However, this problem can be solved with numeric methods, such as a GA based approach [22]. For this work we have adopted a fast and elitist multi-objective genetic algorithm, NSGA-II [23], to calculate the optimum parameters of the model of the gripper. NSGA-II has already been used in similar studies on gripper optimization [6], [19].

The cost function values for the GA based solver were calculated in simulation, using the given parameters. As simulator the freely available MuJoCo [24] simulator was selected for this work, because both it allows simulation of tendons, and it was rated as good in a relevant study [25].

TABLE I: Upper and lower limits of the parameter values.

$\vec{x}$	L_0 (mm)	L_i (mm) $i \in \{1,3,5\}$	L_i (mm) $i \in \{2,4,6\}$	R_i (mm) $i \in \{1..3\}$	H_i (mm) $i \in \{1..3\}$	S_{Ei} $(N.m/rad)$ $i \in \{1..3\}$	S_{Pi} $(N.m/rad)$ $i \in \{1..3\}$	K_i $i \in \{1..3\}$	θ $(^o)$	W (mm)
L.L.	10	5	5	3	-4.5	0	0	-5.5	0	15
U.L.	40	10	20	5	4.5	2	2	5.5	45	15

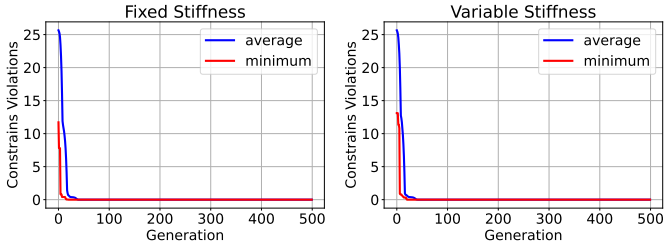

(a) (b)

Fig. 3: Evolution of the constraint violations over the generations of the genetic algorithm for fixed (a) and variable (b) stiffness. Non-zero values indicate infeasible solutions. After the 50^{th} generation, none of the offsprings of the GA leads to infeasible solutions.

In order to use the gripper model with the simulator it was converted to the proper format, representing the bodies, the phalanges, and the components that are doing contact. Then these bodies were connected together and the degrees of freedom of the joints were set. Finally, the connection points of the tendons were specified. Since the used tendons have a constant length, they were connected to a linear displacement actuator, whose actuation force was monitored. To measure the grasping force, force sensors were added to each phalange of the gripper and the palm, giving the forces F_{L_i}, F_{R_i} and F_0 for the left and right phalanges and the palm respectively.

To be able to compare the performance with our previous gripper, the presented optimization algorithm was run for both approaches: fixed and variable stiffness. For fixed stiffness, the method was run by setting $S_{Ei} = S_{Pi}$, maintaining the same stiffness between the different grasp modes.

III. Results

A. Optimization Results

The parameters of the multi-objective genetic algorithm used to solve the above optimization problems, for both fixed and variable stiffness, are the following. The initial population was randomly initialized with a total number of 1000 individuals. The survival of each selected individual depended on the rank and crowding strategy proposed by Kukkonen and Deb [26], and the selection of those individuals was random. The probability of crossover between parents was set to 0.5. Each individual experienced at least one polynomial mutation of the values in each generation of the algorithm, as explained in [27]. Finally, the termination criteria of the algorithm was set to 500 generations.

In Fig. 3, we can observe the evolution of the constraint violation for fixed and variable stiffness over each generation.

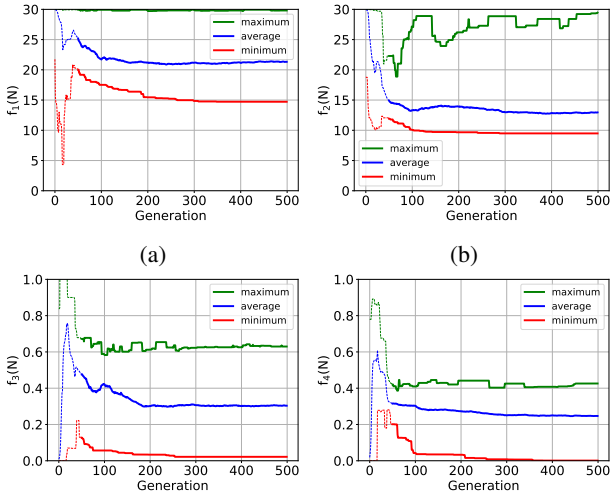

(a) (b) (c) (d)

Fig. 4: Evolution of the objective functions over generations of the genetic algorithm for fixed stiffness.

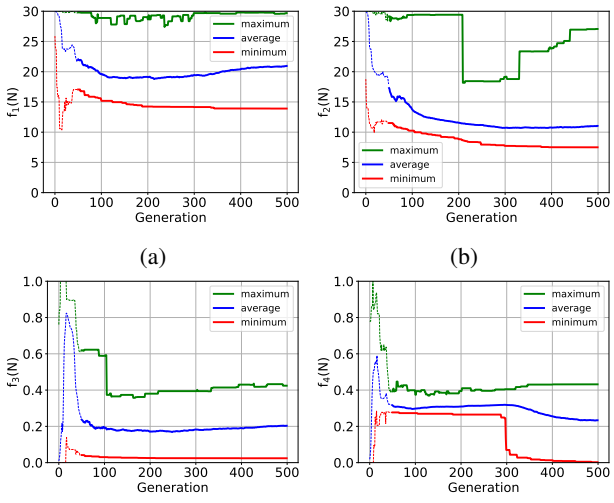

(a) (b) (c) (d)

Fig. 5: Evolution of the objective functions over generations of the genetic algorithm for variable stiffness.

In both cases, the whole populations become feasible solutions very early, around generation 50, but at this point the objective functions had not yet converged as shown in Fig. 4 and Fig. 5. This was the reason to set the termination criteria to a high value at a cost of increased optimization time. The whole optimization process took 10.73 hours for fixed stiffness and 9.38 hours for variable stiffness, while running on a computer

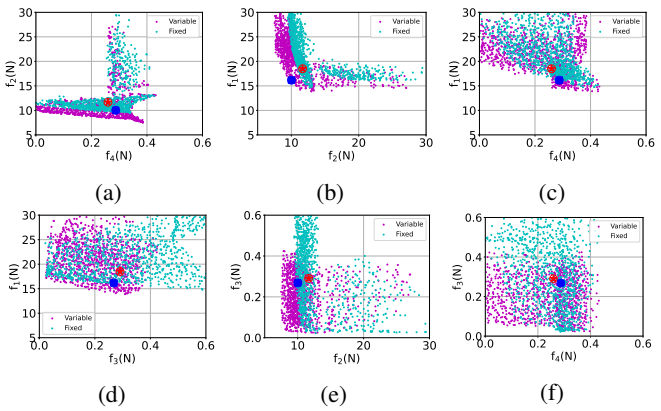

Fig. 6: The cost function values, for variable stiffness (magenta) and fixed stiffness (cyan), of the members of the last population of the GA.

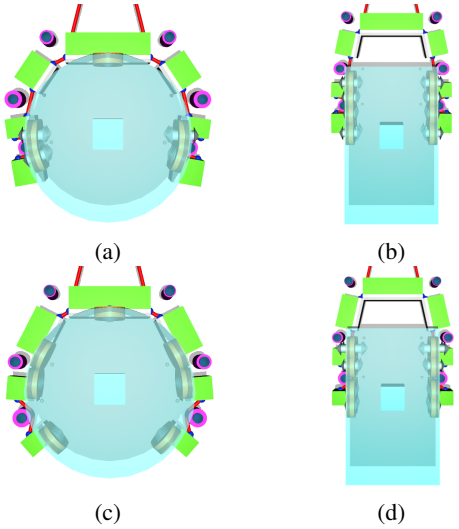

Fig. 7: Simulation of the best result for fixed stiffness while grasping a cylinder (a) and a box (b), and for variable stiffness while grasping a cylinder (c) and a box (d)

with 128GB of memory and 64 cores.

Due to the difficulty of visualizing the 4D objective functions corresponding to the optimization problem, pair-wise 2D plots are shown in Fig. 6, comparing the distributions of the standard deviations of the contact forces and of the actuation forces of both the enveloping grasp and the flat pinching grasp, for fixed and variable stiffness. Overall, we can see that the distributions of the cost functions in the last generations are similar. However, for the variable stiffness case the distributions are closer to the bottom left corner, where the biggest improvement is for f_2. The corresponding distribution is on average $14.83\,\%$ lower than the fixed stiffness case. Therefore, they are better than the fixed stiffness case.

An optimal design would be a point on the lowest left corner of every plot representing a gripper with low actuation force and contact forces uniformly distributed for both grasps. For each problem, the best overall design was chosen to be a configuration where f_3 and f_4 are less than $0.3N$, and the actuation force sum given by $f_1 + f_2$ is minimum. The fixed stiffness could only generate a configuration that achieved minimum actuation forces of $f_1 = 18.5\,\mathrm{N}$ and $f_2 = 11.7\,\mathrm{N}$, whereas the variable stiffness could reduce f_1 down to $16.2\,\mathrm{N}$ and f_2 down to $10.0\,\mathrm{N}$, while both had the standard deviations less than $0.3\,\mathrm{N}$. The resulting design is represented by a red star (fixed stiffness) and blue square (variable stiffness) on each plot (Fig. 6). The corresponding design parameters are presented on the last rows of Table II for the joints and Table III for the lengths and starting angle for fixed stiffness; and on the last rows of Table IV for the joints and Table V for the lengths and starting angle for variable stiffness. In Fig. 7, the resulting designs are shown grasping a box and a cylinder in simulation.

IV. Conclusion

In this work, we improved the design of our previous underactuated gripper [21], by allowing the stiffness of the joints to be variable between different objects in order to achieve the same target contact force with less actuation force over the tendons. Due to the high number of design variables and the multi-objective nature of the proposed cost function, which maximizes the grasping forces for different objects and minimizes the variance of the force at the different phalanges, a Genetic Algorithm was used to solve the problem.

In the transfer of this work to a physical hand some limitations are expected to appear. The friction on the path of the tendons' and the friction on the joints connecting the phalanges are not considered in the simulation. Therefore, it is expected that the ratio of actuation to contact force will increase. Another important limitation is that for the joint stiffness there is no limit defined on the torque, whereas in a real scenario every material has a maximum limit on deformation that it can handle or force that it can apply, so some non-linearity is expected to appear in a physical robot hand. In future works, we will take into account those issues to obtain a more realistic gripper design, and produce a hand with variable stiffness for eventual hardware validation.

References

[1] H. Isakhani, S. Nefti-Meziani, S. Davis, and H. Isakhani, "A bioinspired underactuated dual tendon-based adaptive gripper for space applications," in *2023 IEEE/RSJ International Conference on Intelligent Robots and Systems (IROS)*. IEEE, 2023, pp. 2447–2454.

[2] K. Takács, A. Mason, L. B. Christensen, and T. Haidegger, "Robotic grippers for large and soft object manipulation," in *2020 IEEE 20th international Symposium on computational Intelligence and informatics (CINTI)*. IEEE, 2020, pp. 133–138.

[3] S. Zaidi, M. Maselli, C. Laschi, and M. Cianchetti, "Actuation technologies for soft robot grippers and manipulators: A review," *Current Robotics Reports*, vol. 2, no. 3, pp. 355–369, 2021.

[4] Z. Samadikhoshkho, K. Zareinia, and F. Janabi-Sharifi, "A brief review on robotic grippers classifications," in *2019 IEEE Canadian Conference of Electrical and Computer Engineering (CCECE)*. IEEE, 2019, pp. 1–4.

[5] B. He, S. Wang, and Y. Liu, "Underactuated robotics: a review," *International Journal of Advanced Robotic Systems*, vol. 16, no. 4, p. 1729881419862164, 2019.

TABLE II: Optimization results for the joint related variables for fixed stiffness.

	R_1 (mm)	H_1 (mm)	S_{E1}/S_{P1} $(N.m/rad)$	K_1 (mm)	R_2 (mm)	H_2 (mm)	S_{E2}/S_{P2} $(N.m/rad)$	K_2 (mm)	R_3 (mm)	H_3 (mm)	S_{E3}/S_{P3} $(N.m/rad)$	K_3 (mm)
Average	3.90	-4.40	0.010	5.48	3.58	-2.57	0.102	4.95	3.27	0.25	0.230	0.29
StdDev	0.50	0.27	0.001	0.05	0.40	2.00	0.075	0.60	0.50	1.45	0.439	2.81
Best	3.50	-4.50	0.010	5.50	4.00	-3.60	0.049	3.20	3.00	-0.40	0.010	2.30

TABLE III: Optimization results for lengths and starting angle for fixed stiffness

	L_0 (mm)	L_1 (mm)	L_2 (mm)	L_3 (mm)	L_4 (mm)	L_5 (mm)	L_6 (mm)	W (mm)	θ $(^o)$
Average	22.31	9.99	8.26	9.06	6.11	9.65	15.75	15	44.24
StdDev	1.22	0.04	2.52	1.27	1.06	0.67	5.56	0	1.05
Best	22.10	10.00	7.70	7.50	5.00	9.50	18.50	15	44.50

TABLE IV: Optimization results for the joint related variables for variable stiffness.

	R_1 (mm)	H_1 (mm)	S_{E1} $(N.m/rad)$	S_{P1} $(N.m/rad)$	K_1 (mm)	R_2 (mm)	H_2 (mm)	S_{E2} $(N.m/rad)$	S_{P2} $(N.m/rad)$	K_2 (mm)	R_3 (mm)	H_3 (mm)	S_{E3} $(N.m/rad)$	S_{P3} $(N.m/rad)$	K_3 (mm)
Average	3.54	-4.49	0.013	0.004	5.49	4.33	-4.01	0.013	0.217	5.32	4.70	1.35	0.100	1.911	-3.97
StdDev	0.31	0.05	0.046	0.012	0.04	0.39	0.64	0.015	0.096	0.19	0.61	1.02	0.273	0.107	1.62
Best	3.20	-4.50	0.151	0.000	5.50	3.10	-4.50	0.000	0.077	5.40	4.90	1.40	0.000	1.901	-5.50

TABLE V: Optimization results for lengths and starting angle for variable stiffness

	L_0 (mm)	L_1 (mm)	L_2 (mm)	L_3 (mm)	L_4 (mm)	L_5 (mm)	L_6 (mm)	W (mm)	θ $(^o)$
Average	19.86	9.97	11.92	8.68	9.81	9.48	5.66	15	44.80
StdDev	2.01	0.10	3.98	1.37	1.34	0.43	0.82	0	0.46
Best	15.00	10.00	6.20	10.00	9.80	9.90	5.10	15	45.00

[6] R. Datta, S. Pradhan, and B. Bhattacharya, "Analysis and design optimization of a robotic gripper using multiobjective genetic algorithm," *IEEE Transactions on Systems, Man, and Cybernetics: Systems*, vol. 46, no. 1, pp. 16–26, 2015.

[7] T. Chen, Z. He, and M. Ciocarlie, "Hardware as policy: Mechanical and computational co-optimization using deep reinforcement learning," in *Conference on Robot Learning*. PMLR, 2021, pp. 1158–1173.

[8] Z. Zhang, Y. Zheng, Z. Hu, L. Liu, X. Zhao, X. Li, and J. Pan, "A computational framework for robot hand design via reinforcement learning," in *2021 IEEE/RSJ international conference on intelligent robots and systems (IROS)*. IEEE, 2021, pp. 7216–7222.

[9] T. Treratanakulwong, H. Kaminaga, and Y. Nakamura, "Low-friction tendon-driven robot hand with carpal tunnel mechanism in the palm by optimal 3d allocation of pulleys," in *2014 IEEE International Conference on Robotics and Automation (ICRA)*. IEEE, 2014, pp. 6739–6744.

[10] J.-M. Boisclair, T. Laliberté, and C. Gosselin, "On the optimal design of underactuated fingers using rolling contact joints," *IEEE Robotics and Automation Letters*, vol. 6, no. 3, pp. 4656–4663, 2021.

[11] S. J. Yoon, M. Choi, B. Jeong, and Y.-L. Park, "Elongatable gripper fingers with integrated stretchable tactile sensors for underactuated grasping and dexterous manipulation," *IEEE Transactions on Robotics*, vol. 38, no. 4, pp. 2179–2193, 2022.

[12] I. Hussain, G. Salvietti, M. Malvezzi, and D. Prattichizzo, "On the role of stiffness design for fingertip trajectories of underactuated modular soft hands," in *2017 IEEE International Conference on Robotics and Automation (ICRA)*. IEEE, 2017, pp. 3096–3101.

[13] B. Yang, L. Jiang, G. Bao, H. Yu, and X. Zhou, "Co-optimization of robotic design and skill inspired by human hand evolution," *Bioinspiration & Biomimetics*, vol. 18, no. 1, p. 016002, 2022.

[14] Y. Zhang, D. Xia, Q. Lu, Q. Zhang, H. Wei, and W. Chen, "Design, analysis and experimental research of dual-tendon-driven underactuated gripper," *Machines*, vol. 10, no. 9, p. 761, 2022.

[15] K. Mizushima, T. Oku, Y. Suzuki, T. Tsuji, and T. Watanabe, "Multi-fingered robotic hand based on hybrid mechanism of tendon-driven and jamming transition," in *2018 IEEE International Conference on Soft Robotics (RoboSoft)*. IEEE, 2018, pp. 376–381.

[16] W. Wang, C. Y. Yu, P. A. Abrego Serrano, and S.-H. Ahn, "Shape memory alloy-based soft finger with changeable bending length using targeted variable stiffness," *Soft robotics*, vol. 7, no. 3, pp. 283–291, 2020.

[17] Y. Yang, Y. Chen, Y. Li, Z. Wang, and Y. Li, "Novel variable-stiffness robotic fingers with built-in position feedback," *Soft robotics*, vol. 4, no. 4, pp. 338–352, 2017.

[18] M. Ciocarlie and P. Allen, "Data-driven optimization for underactuated robotic hands," in *2010 IEEE International Conference on Robotics and Automation*. IEEE, 2010, pp. 1292–1299.

[19] H. Dong, E. Asadi, C. Qiu, J. Dai, and I.-M. Chen, "Geometric design optimization of an under-actuated tendon-driven robotic gripper," *Robotics and Computer-Integrated Manufacturing*, vol. 50, pp. 80–89, Apr. 2018.

[20] V. Bo, E. Turco, M. Pozzi, M. Malvezzi, and D. Prattichizzo, "A data-driven topology optimization framework for designing robotic grippers," in *2023 IEEE International Conference on Soft Robotics (RoboSoft)*. IEEE, 2023, pp. 1–6.

[21] D. Denizon, S. Dogru, and L. Marques, "Optimization of an underactuated two finger robotic hand using genetic algorithms," in *Climbing and Walking Robots, CLAWAR2024*, Sep. 2024.

[22] P. Mohapatra, S. Roy, K. N. Das, S. Dutta, and M. S. S. Raju, "A review of evolutionary algorithms in solving large scale benchmark optimisation problems," *International Journal of Mathematics in Operational Research*, vol. 21, no. 1, pp. 104–126, 2022.

[23] K. Deb, A. Pratap, S. Agarwal, and T. Meyarivan, "A fast and elitist multiobjective genetic algorithm: Nsga-ii," *IEEE transactions on evolutionary computation*, vol. 6, no. 2, pp. 182–197, 2002.

[24] E. Todorov, T. Erez, and Y. Tassa, "Mujoco: A physics engine for model-based control," in *2012 IEEE/RSJ international conference on intelligent robots and systems*. IEEE, 2012, pp. 5026–5033.

[25] T. Erez, Y. Tassa, and E. Todorov, "Simulation tools for model-based robotics: Comparison of bullet, havok, mujoco, ode and physx," in *2015 IEEE international conference on robotics and automation (ICRA)*. IEEE, 2015, pp. 4397–4404.

[26] S. Kukkonen and K. Deb, "A fast and effective method for pruning of non-dominated solutions in many-objective problems," in *International conference on parallel problem solving from nature*. Springer, 2006, pp. 553–562.

[27] K. Deb, K. Sindhya, and T. Okabe, "Self-adaptive simulated binary crossover for real-parameter optimization," in *Proceedings of the 9th annual conference on genetic and evolutionary computation*, 2007, pp. 1187–1194.